Supporting Information for

Cerium-Carbon Dative Interactions Supported by Carbodiphosphorane

Wei Su,[a] Sudip Pan,[b] Xiong Sun,[a] Lili Zhao,*[b] Gernot Frenking,*[b,c,d] and Congqing Zhu*[a]

[a] State Key Laboratory of Coordination Chemistry, Jiangsu Key Laboratory of Advanced Organic Materials, School of Chemistry and Chemical Engineering, Nanjing University, Nanjing 210093, China

[b] Institute of Advanced Synthesis, School of Chemistry and Molecular Engineering, Jiangsu National Synergetic Innovation Center for Advanced Materials, Nanjing Tech University, Nanjing 211816, China

[c] Fachbereich Chemie, Philipps-Universität Marburg, Hans-Meerwein-Straße 4, Marburg 35032, Germany

[d] Donostia International Physics Center (DIPC), P.K. 1072, 20080 Donostia, Euskadi, Spain.

* Correspondence and requests for materials should be addressed to C.Z. (zcq@nju.edu.cn) or to L.Z. (ias_llzhao@njtech.edu.cn) or to G.F. (frenking@chemie.uni-marburg.de).

Contents

1. Experimental section

General procedures: Synthesis of cerium complexes was carried out in a glove-box (SG1800/750TS-F, VIGOR) under an N_2 atmosphere with O_2 and H_2O content both less than 1 ppm. The solvents were obtained by passing through a Solv Purer G5 (MIKROUNA) solvent purification system and further dried over 4 Å molecular sieves. C_6D_6 was distilled over Na and benzophenone and stored under N_2 prior to use. Deuterated dichloromethane (DCM-d_2) was distilled from CaH_2 and stored under an N_2 atmosphere prior to use. Other reagents were used as received without further purification. The nuclear magnetic resonance spectra were recorded at room temperature (RT) on a Bruker AVIII-400 (^{1}H 400.1 MHz; ^{31}P{^{1}H} 162.0 MHz) spectrometer. ^{1}H NMR chemical shifts are referred to an internal standard, tetramethylsilane, and ^{31}P{^{1}H} NMR chemical shifts are relative to 85% H_3PO_4. Elemental analysis (C, H, N) was performed on a Vario EL III elemental analyser at the Shanghai Institute of Organic Chemistry, the Chinese Academy of Sciences. FT-IR was performed with a Bio-Rad FTS-185 spectrometer. Compound [H_2**1**](PF_6)$_2$ was synthesized as previously reported.[1]

Synthesis of ligand 1.

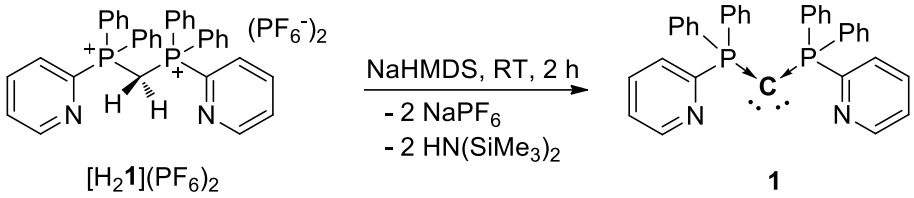

A solution of NaHMDS in THF (2 M, 3 mL) was added dropwise to an off-white suspension of $[H_2\mathbf{1}](PF_6)_2$ (3 mmol, 2.49 g) in THF (15 mL), producing a dark brown solution which was then stirred at RT for 2 h. Subsequently, it was concentrated to *ca.* 5 mL and stored overnight at -30 ^{o}C. The yellow solid was collected by decanting the mother liquid and then was washed with cold THF (1 mL × 3), and dried in *vacuo*. Yield: 1.10 g, 68%. ^{1}H NMR (400 MHz, Benzene-d_6, 298 K) δ 8.70 (dt, *J* = 7.2, 3.3 Hz, 2H, Py), 8.35 (d, *J* = 4.0 Hz, 2H, Py), 8.07 (m, 8H, Ph), 7.11 – 6.93 (m, 14H, Py+Ph), 6.50 (dd, *J* = 7.8, 4.8, 2H, Py). ^{13}C{^{1}H} NMR (101 MHz, Benzene-d_6, 298 K): δ 148.7 (t, *J* = 9.1Hz), 134.6 (t, *J* = 4.0 Hz), 132.6 (t, *J* = 5.1 Hz), 129.0 (s), 128.4 (t, *J* = 11.1 Hz), 127.3 (t, *J* = 6.1 Hz), 122.6 (s). ^{31}P{^{1}H} NMR (162 MHz, Benzene-d_6, 298 K) δ -5.1 (s).

Synthesis of complex 2

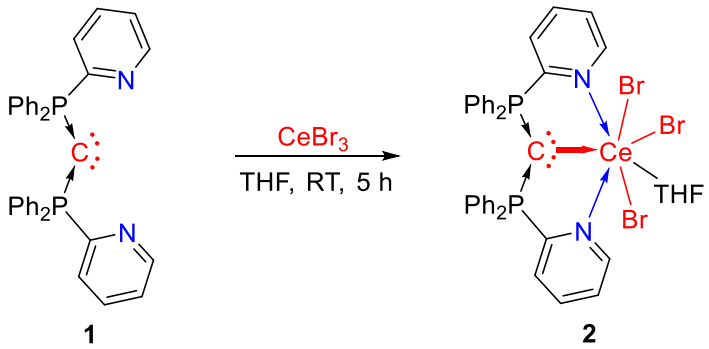

THF (20 mL) was added to a mixture of **1** (0.5 mmol, 270 mg) and $CeBr_3$ (0.5 mmol,

190 mg). The yellow suspension was stirred at RT for 5 h. It was then filtered and the yellow residue on Celite was thoroughly washed with THF (5 mL × 3). Subsequently, the yellow residue was dissolved in DCM to give a yellow solution. The filtrate was dried in *vacuo*, affording the desired product as yellow powder. Crystals suitable for X-ray analysis were obtained by diffusion of Et_2O into a saturated DCM solution of **2**. Yield: 470 mg, 95%. ^{1}H NMR (400 MHz, DCM-d_2, 298 K): δ 10.65, 8.32, 7.91, 7.76, 6.46, 4.06, 3.19, 2.11, -10.71 ppm. ^{31}P{^{1}H} NMR (162 MHz, DCM-d_2, 298 K): -10.2 ppm. Anal. calcd. for **2** ·CH_2Cl_2 ($C_{40}H_{38}Br_3Cl_2CeN_2OP_2$): C, 44.67; H, 3.56; N, 2.60. Found: C, 45.09; H, 3.60; N, 2.53. FT-IR ν/cm^{-1} (Nujol): 1622 (w), 1571 (w), 1439 (s), 1214 (w), 1105 (m), 988 (m), 744 (m), 729 (m), 716 (m), 690 (m), 560 (m), 528 (m), 498 (m).

Synthesis of complex 3.

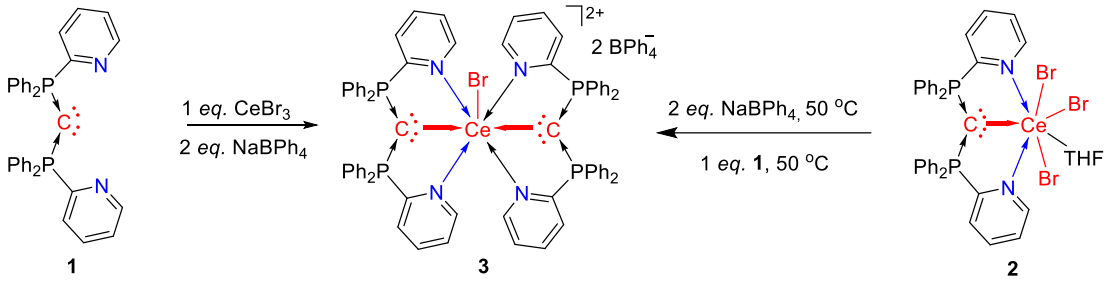

A suspension of **1** (0.5 mmol, 270 mg), $CeBr_3$ (0.25 mmol, 95 mg) and $NaBPh_4$ (0.5 mmol, 171 mg) in THF was stirred at RT for 8 h. The resulting suspension was then filtered and the yellow residue over Celite was thoroughly washed with THF (5 ml × 3). Subsequently, the yellow residue was dissolved in DCM to give a yellow-orange solution. The filtrate was dried *in vacuo*, affording the desired product as a yellow-orange powder. Orange crystals suitable for X-ray analysis were obtained by

slow evaporation of Et_2O into a saturated solution of **3** in DCM. Yield: 321 mg, 66%.

Alternatively, **3** could be prepared stepwise. A suspension of **2** (0.5 mol, 495 mg) and $NaBPh_4$ (1 mmol, 342 mg) in THF (5 mL) was stirred at 50 ^oC for 30 min, when the solution became yellow. Compound **1** (0.5 mmol, 270 mg) in THF (5 mL) was then added and the mixture was stirred at 50 ^oC for a further 12 h, affording a yellow suspension. Work-up was the same as in the previous method. Yield: 730 mg, 78%. Once obtained in its crystalline form, redissolvation of complex **3** with polar solvent (DCM, pyridine, *etc.*) would lead to its complete decomposition. The low stability of complex **3** in solution prevented reliable characterizations, but the isolation of **3** was repeated three times and the products' solid structures were identical. Anal. Calcd. for **3**·CH_2Cl_2 ($C_{119}H_{98}B_2BrCl_2CeN_4P_4$): C, 70.74; H, 4.89; N, 2.77. Found: C, 70.71; H, 4.97; N, 2.69. FT-IR ν/cm^{-1} (Nujol): 1715 (w), 1578 (m), 1437 (s), 1425 (s), 1311 (w), 1266 (w), 1211 (w), 1152 (m), 1136 (m), 1122 (m), 1104 (m), 1069 (w), 1048 (w), 1031 (w), 989 (m), 844 (w), 805 (w), 769 (w), 733 (s), 705 (s), 693 (s), 613 (m), 554 (m), 540 (m), 528 (m), 499 (m).

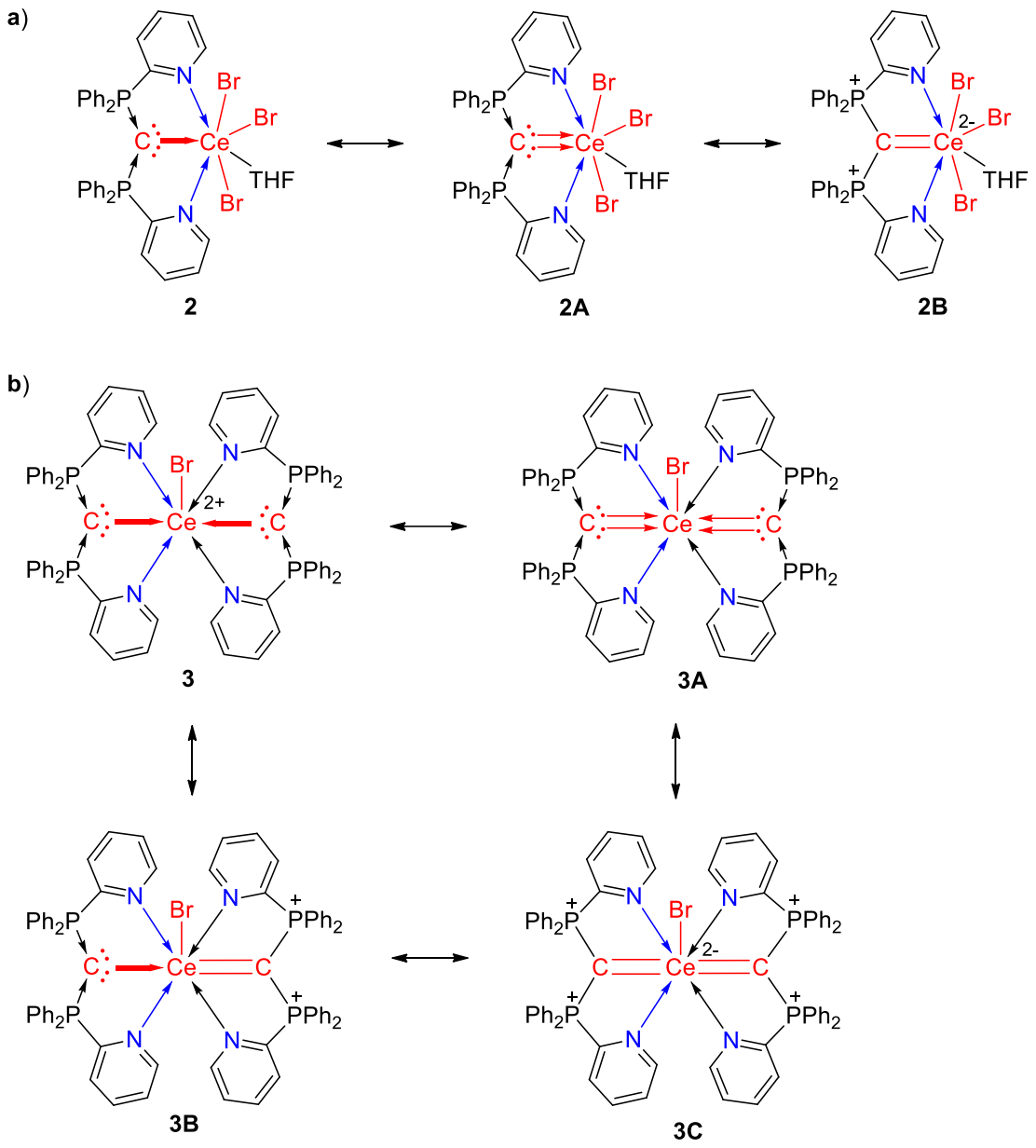

Figure S1. Major resonance structures of complex **2** (**a**) and the cation of complex **3** (**b**).

2. NMR spectra

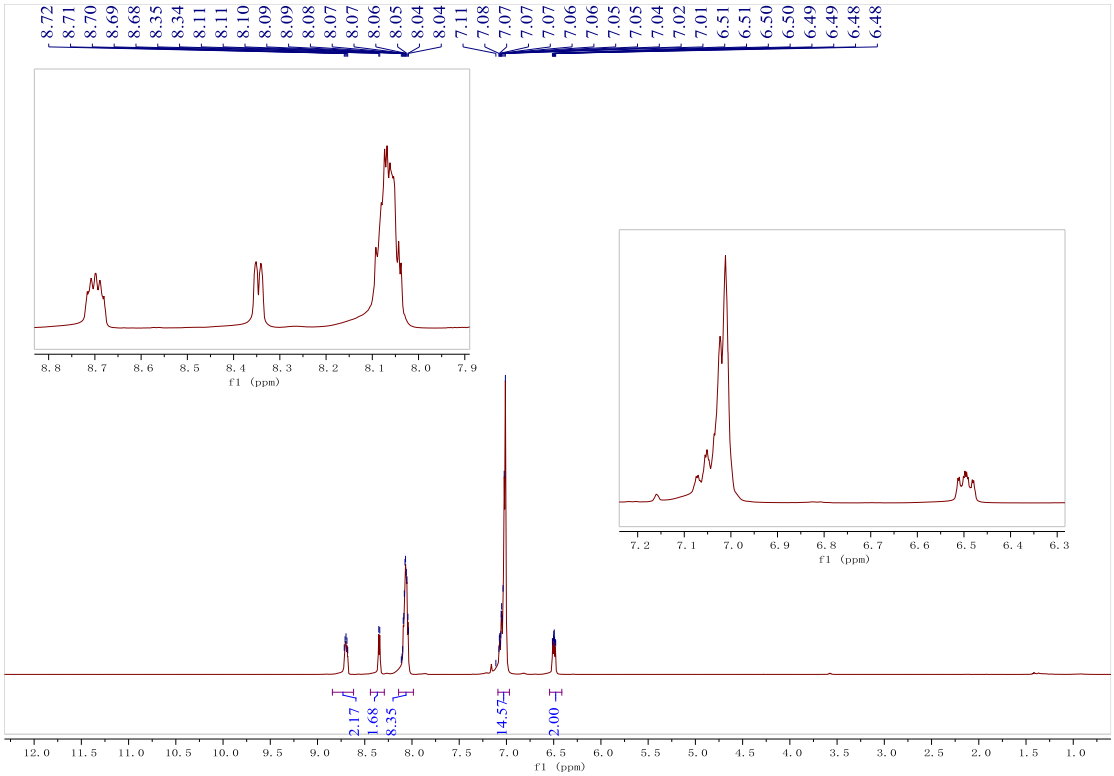

Figure S2. ^{1}H NMR of complex **1** in C_6D_6.

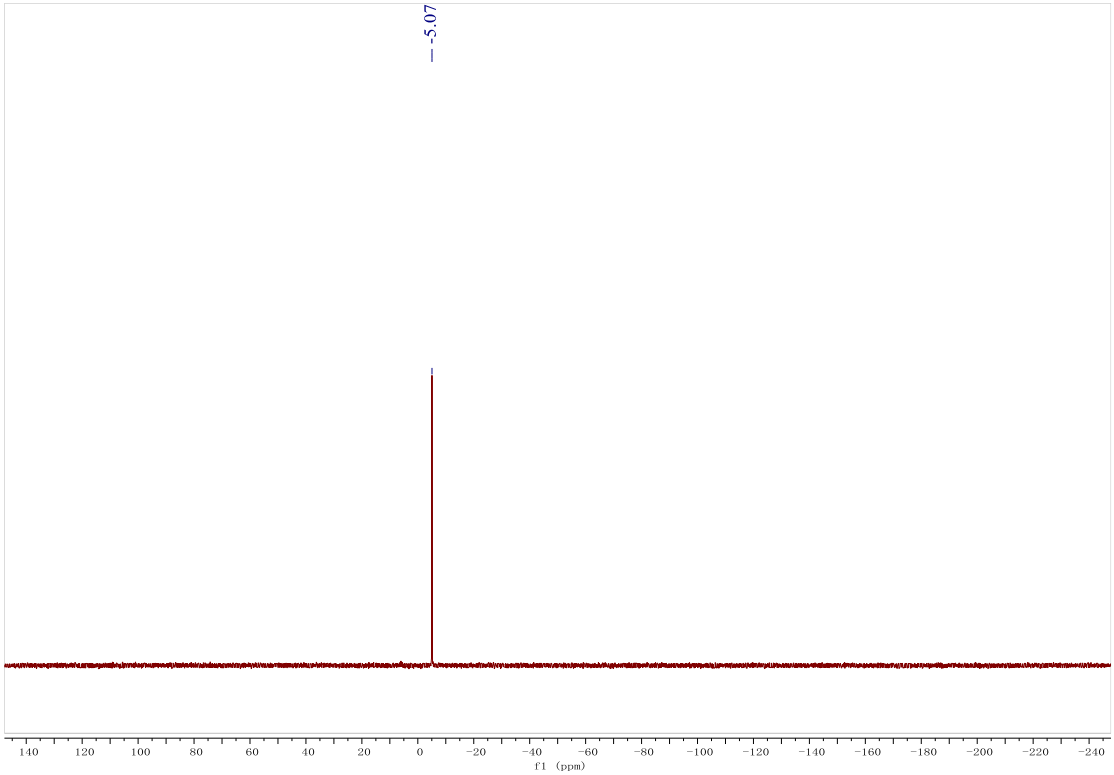

Figure S3. ^{31}P{^{1}H} NMR spectra of complex **1** in C_6D_6.

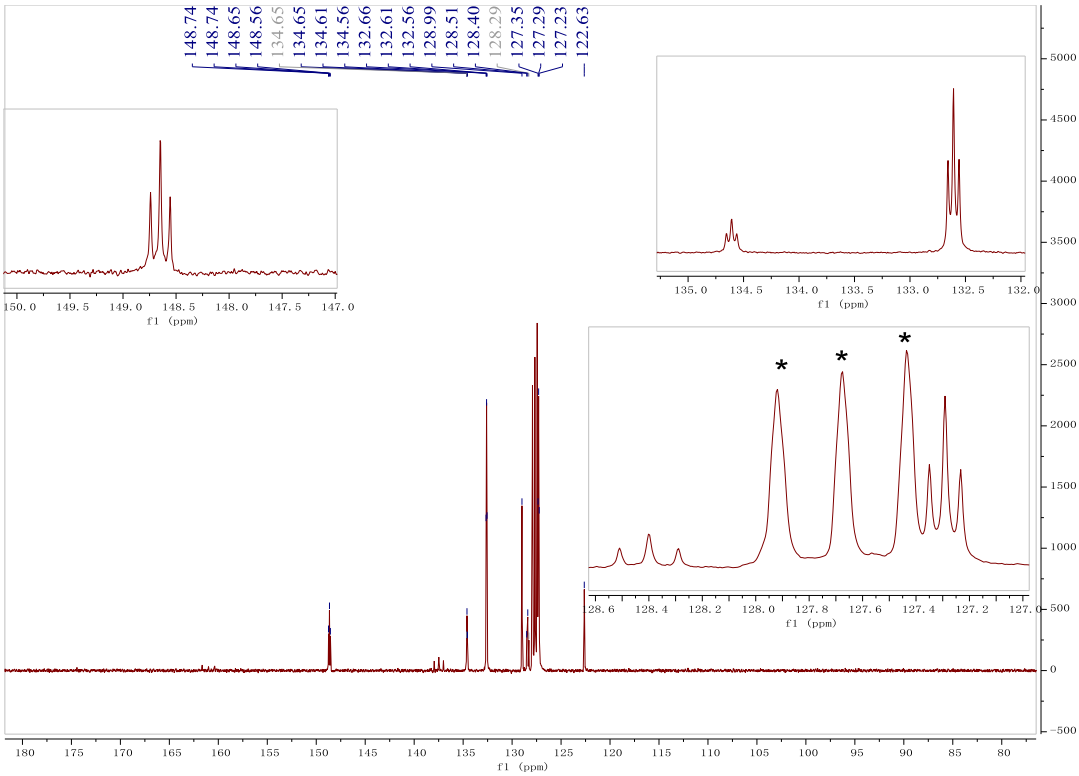

Figure S4. $^{13}C\{^{1}H\}$ NMR spectra of complex **1** in C_6D_6 (*, solvent residue peak).

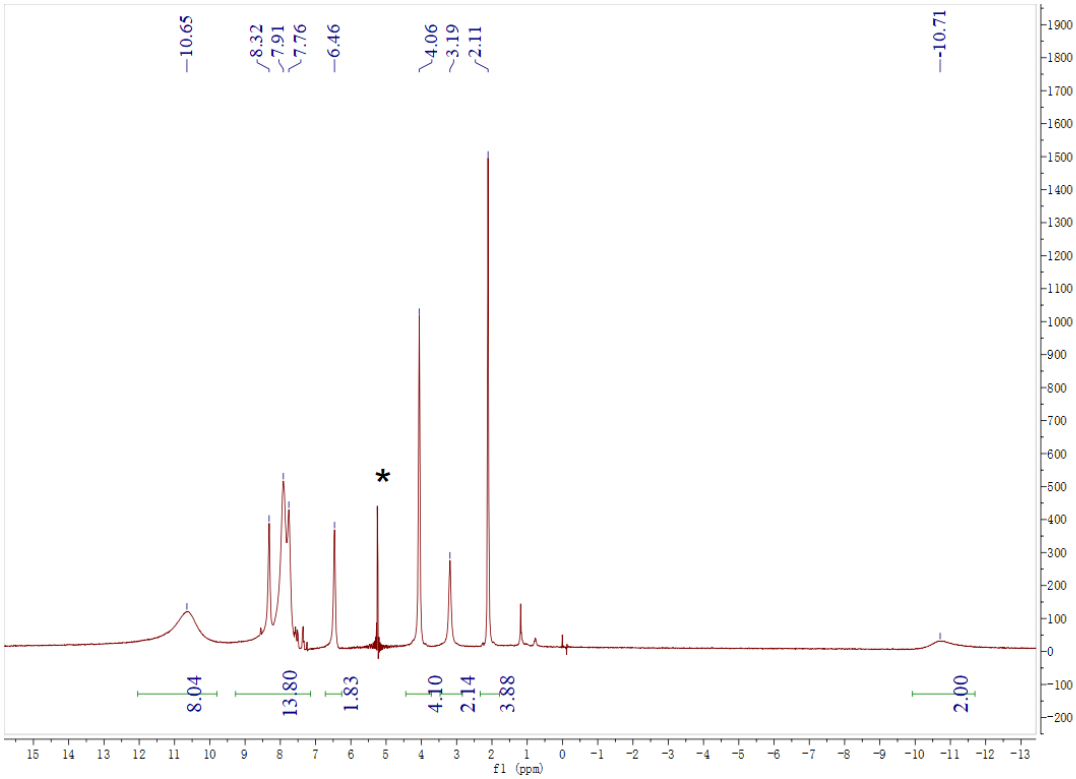

Figure S5. ^{1}H NMR of complex **2** in DCM-d_2 (*, solvent residue peak).

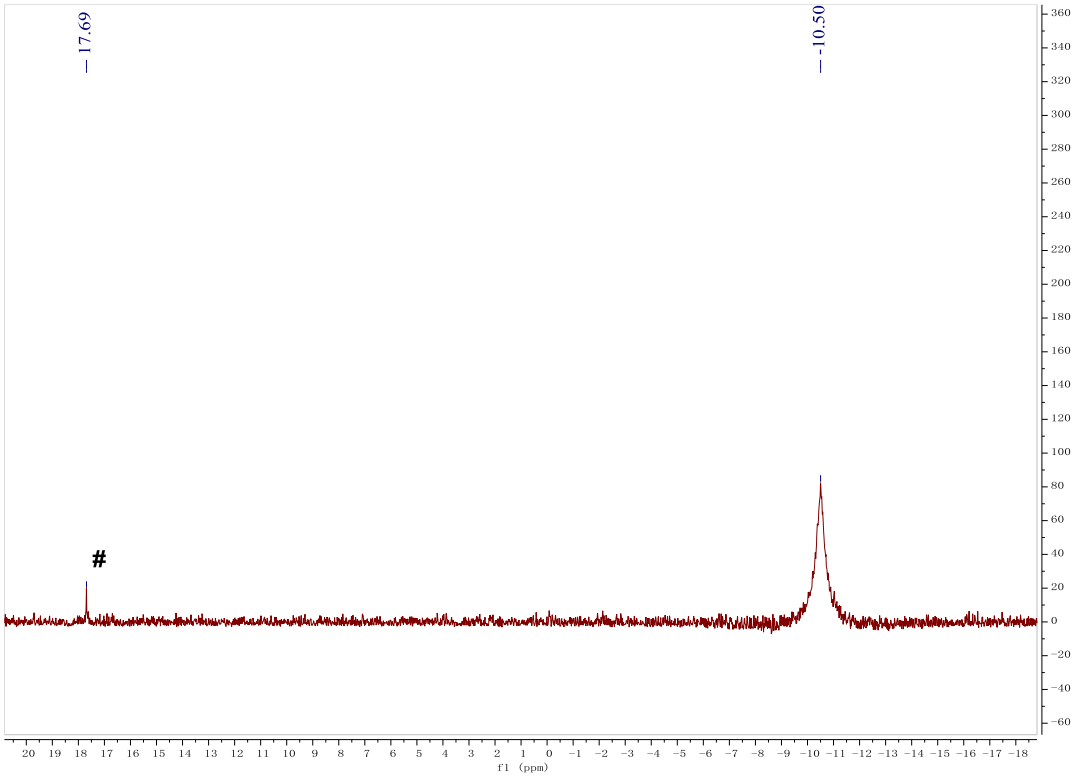

Figure S6. $^{31}P\{^{1}H\}$ NMR spectra of complex **2** in DCM-d_2(#, protonated **1**).

3. X-ray Crystallography

Crystals suitable for X-ray diffraction were obtained by slow evaporation of Et_2O into a saturated solution of complexes **2** and **3** in DCM. The intensity data were collected with a Bruker APEX-II CCD area detector using graphite-monochromated Mo Kα radiation (λ = 0.71073 Å) or Ga Kα radiation (λ = 0.134139 Å). Multiscan or empirical absorption corrections (SADABS) were applied. The structures were solved by Patterson methods, expanded by difference Fourier syntheses, and refined by full-matrix least squares on F^2 using the Bruker SHELXTL-2014 program package.[2] All non-hydrogen atoms were refined anisotropically. Hydrogen atoms were introduced at their geometric positions and refined as riding atoms. The X-ray crystal structures have been deposited in the Cambridge Crystallographic Data Centre (CCDC) and the data can be obtained free of charge from the CCDC (www.ccdc.cam.ac.uk/data_request/cif). Details of the data collection and refinement for complexes **2** and **3** are given in Tables S1 and S2.

Table S1. Crystal data and structure refinement for **2** ·2CH_2Cl_2.

CCDC number	1919789
Empirical formula	$C_{41}H_{40}Br_3CeCl_4N_2OP_2$
Formula weight	1160.34
Temperature/K	153
Crystal system	triclinic
Space group	P-1
a/Å	11.4475(6)
b/Å	12.6572(7)
c/Å	16.0775(9)
α/°	77.950(2)
β/°	87.542(2)
γ/°	73.331(2)
Volume/$Å^3$	2182.1(2)
Z	2
ρ_{calc}g/cm^3	1.766
μ/mm^{-1}	4.143
F(000)	1138.0
Crystal size/mm^3	0.05 ×0.04 ×0.03
Radiation	MoKα (λ = 0.71073)
2Θ range for data collection/°	4.282 to 49.998
Index ranges	$-13 \leq h \leq 13$, $-15 \leq k \leq 11$, $-19 \leq l \leq 18$
Reflections collected	16087
Independent reflections	7648 [R_{int} = 0.0434, R_{sigma} = 0.0652]
Data/restraints/parameters	7648/20/497
Goodness-of-fit on F^2	1.045
Final R indexes [I>=2σ (I)]	R_1 = 0.0494, wR_2 = 0.1236
Final R indexes [all data]	R_1 = 0.0683, wR_2 = 0.1303
Largest diff. peak/hole / e $Å^{-3}$	2.34/-1.93

Table S2. Crystal data and structure refinement for **3**.

CCDC number	1919790	1919791	1919792
Empirical formula	$C_{118}H_{96}B_2BrCeN_4P_4$		
Formula weight	1935.51		
Temperature/K	153	193	193
Crystal system	monoclinic		
Space group	$P2_1/c$		
a/Å	17.1745(11)	17.0971(11)	17.131
b/Å	29.9779(17)	30.3657(18)	30.502
c/Å	19.4419(13)	19.5806(13)	19.646
α/°	90	90	90
β/°	105.349(2)	104.649(3)	104.62
γ/°	90	90	90
Volume/$Å^3$	9652.7(11)	9835.1(11)	9932.7
Z	4	4	4
ρ_{calc}g/cm^3	1.332	1.307	1.294
μ/mm^{-1}	1.005	3.437	3.307
F(000)	3980.0	3980.0	3980.0
Crystal size/mm^3	0.05 × 0.04 × 0.03	0.06 × 0.04 × 0.03	0.2 × 0.1 × 0.05
Radiation	MoKα (λ = 0.71073)	GaKα (λ = 1.34139)	GaKα (λ = 1.34139)
2Θ range for data collection/ °	4.39 to 50.054	4.648 to 105.96	4.638 to 108.02
Index ranges	-20 ≤ h ≤ 20, -35 ≤ k ≤ 35, -23 ≤ l ≤ 20	-20≤ h ≤ 20, -30≤ k ≤ 36, -23 ≤ l ≤ 23	-20≤ h ≤ 20, -36≤ k ≤ 25, -14 ≤ l ≤ 23
Reflections collected	141612	90872	86025
Independent reflections	17059 [R_{int} = 0.1170, R_{sigma} = 0.0745]	17341 [R_{int} = 0.0634, R_{sigma} = 0.0423]	18140[R_{int} = 0.1390, R_{sigma} = 0.1205
Data/restraints/parameters	17059/0/1171	17341/0/1208	18140/30/1208
Goodness-of-fit on F^2	1.166	1.052	1.023
Final R indexes [I>=2σ (I)]	R_1 = 0.0786, wR_2 = 0.1458	R_1 = 0.0464, wR_2 = 0.1156	R_1 = 0.0675, wR_2 = 0.1512
Final R indexes [all data]	R_1 = 0.1222, wR_2 = 0.1649	R_1 = 0.0542, wR_2 = 0.1197	R_1 = 0.1456, wR_2 = 0.1874
Largest diff. peak/hole / e $Å^{-3}$	1.57/-0.85	1.94/-0.89	1.52/-1.05

4. Computational Details and Supplementary Data.

Computational details: The geometries of **2** and **3** in their doublet and quartet spin states were fully optimized at the BP86-D3(BJ)/def2-SVP/Stuttgart RSC ECP level[3,4] where Stuttgart RSC ECP basis set is used for Ce and def2-SVP is used for other elements. Taking the most stable doublet complex for **2**, further reoptimization was performed at the BP86-D3(BJ)/def2-TZVPP/Stuttgart RSC ECP level. Harmonic vibrational frequency calculations were also done to learn the nature of the stationary points, the zero-point energy (ZPE) and free energy values. The Stuttgart RSC ECP basis set considers quasi-relativistic effective core potential (ECP) for 28 core electrons. The correction to basis set superposition error (BSSE) is incorporated by using the standard counterpoise (CP) method proposed by Boys and Bernardi.[5] All these computations were done using the Gaussian 16 program.[6] The partial charges on each atom of the complexes were computed via natural bond orbital (NBO) analysis using NBO 7.0 program.[7] Quantum theory of atoms in molecules (QTAIM) analysis was performed with wave functions generated at the BP86-D3(BJ)/def2-TZVPP/x2c-TZVPPall[8] level (for **2**) and BP86-D3(BJ)/def2-SVP/x2c-TZVPPall (for **3**) level using the AIMALL program[9] where all electron x2c-TZVPPall basis set is used for Ce instead of ECP. The EDA-NOCV[10] was carried out using ADF(2017.01) program package[11] at the BP86-D3(BJ)/TZ2P-ZORA level[12] where the scalar relativistic effects were considered for Ce using the zeroth-order regular approximation (ZORA).[13] In EDA, the interaction energy (ΔE_{int}) between two fragments is decomposed into four energy terms, viz., the electrostatic interaction energy (ΔE_{elstat}), the Pauli repulsion (ΔE_{Pauli}), the orbital interaction energy (ΔE_{orb}), and the dispersion interaction energy (ΔE_{disp}), Therefore, the interaction energy (ΔE_{int}) between two fragments can be defined as:

$$\Delta E_{\text{int}} = \Delta E_{\text{elstat}} + \Delta E_{\text{Pauli}} + \Delta E_{\text{orb}} + \Delta E_{\text{disp}} \qquad (1).$$

where ΔE_{elstat} is computed classically by taking the two fragments at their optimized positions but considering the charge distribution is unperturbed on each fragment by other one. The next one is ΔE_{Pauli}, which appears as the repulsive energy between

electrons of the same spin and it is computed by employing Kohn-Sham determinant on the superimposed fragments to obey the Pauli principle by antisymmetrization and renormalization. The ΔE_{orb} originates from the mixing of orbitals, charge transfer and polarization between two fragments. Finally, the ΔE_{disp} represents the dispersion interaction between the two fragments.

The EDA-NOCV calculation combines charge and energy decomposition schemes to divide the deformation density, $\Delta\rho(r)$, associated with the bond formation into different components (σ, π, δ) of a chemical bond. From the mathematical point of view, each NOCV, ψ_i is defined as an eigenvector of the deformation density matrix in the basis of fragment orbitals.

$$\Delta P \psi_i = v_i \psi_i \qquad (2).$$

In EDA-NOCV, ΔE_{orb} is given by the following equation

$$\Delta E_{orb} = \sum_k \Delta E_k^{orb} = \sum_{k=1}^{N/2} v_k [-F_{-k}^{TS} + F_k^{TS}] \qquad (3),$$

where, $-F_{-k}^{TS}$ and F_k^{TS} are diagonal Kohn-Sham matrix elements corresponding to NOCVs with the eigenvalues $-v_k$ and v_k, respectively. The ΔE_k^{orb} terms are assigned to a particular type of bond by visual inspection of the shape of the deformation density, $\Delta\rho_k$. The EDA-NOCV scheme thus provides both qualitative ($\Delta\rho_{orb}$) and quantitative (ΔE_{orb}) information about the strength of orbital interactions in chemical bonds. More details about EDA-NOCV can be found in related reviews.[14]

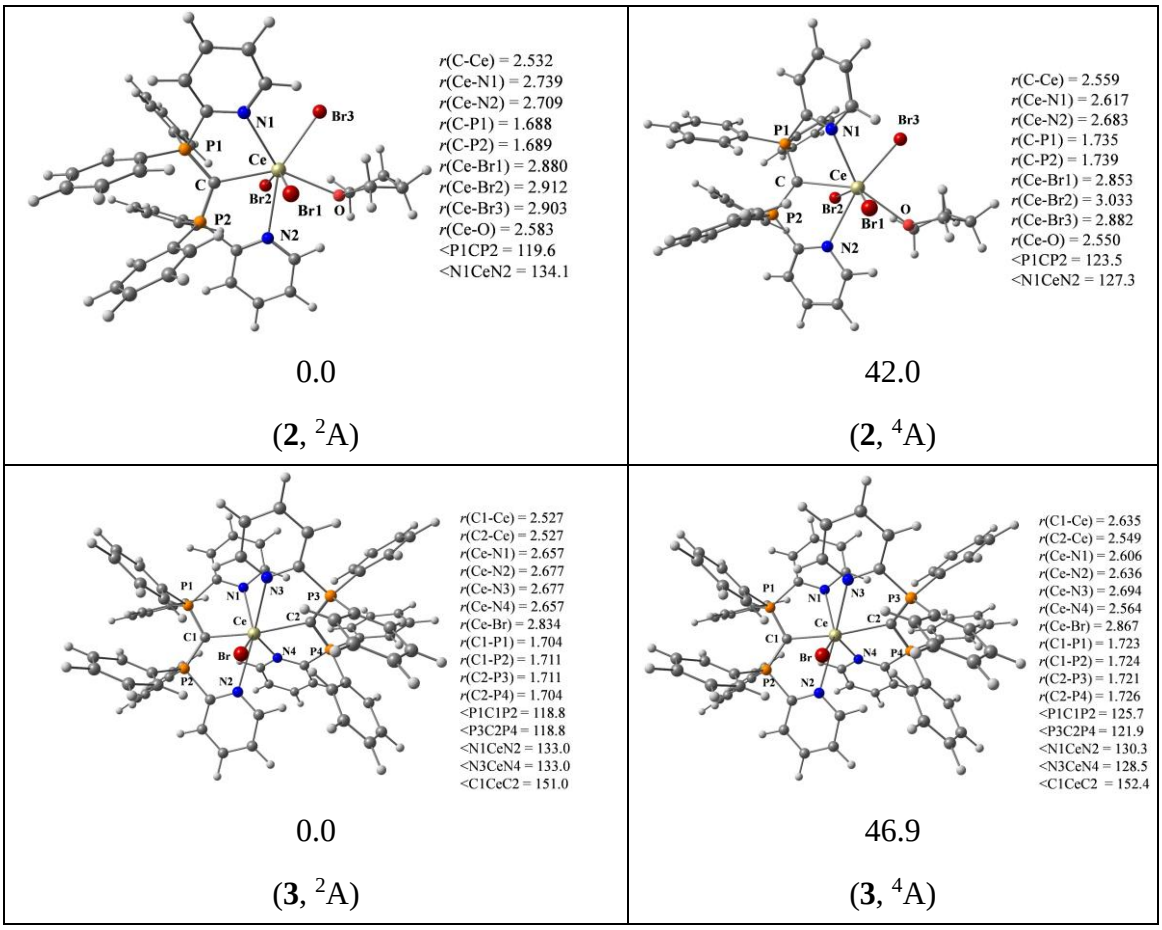

Figure S7. The BP86-D3(BJ)/def2-SVP/Stuttgart RSC 1997 ECP geometries of **2** and **3** in doublet and quartet states. The bond distances and angles are in Å and degree, respectively. Relative energies are in kcal mol^{-1}.

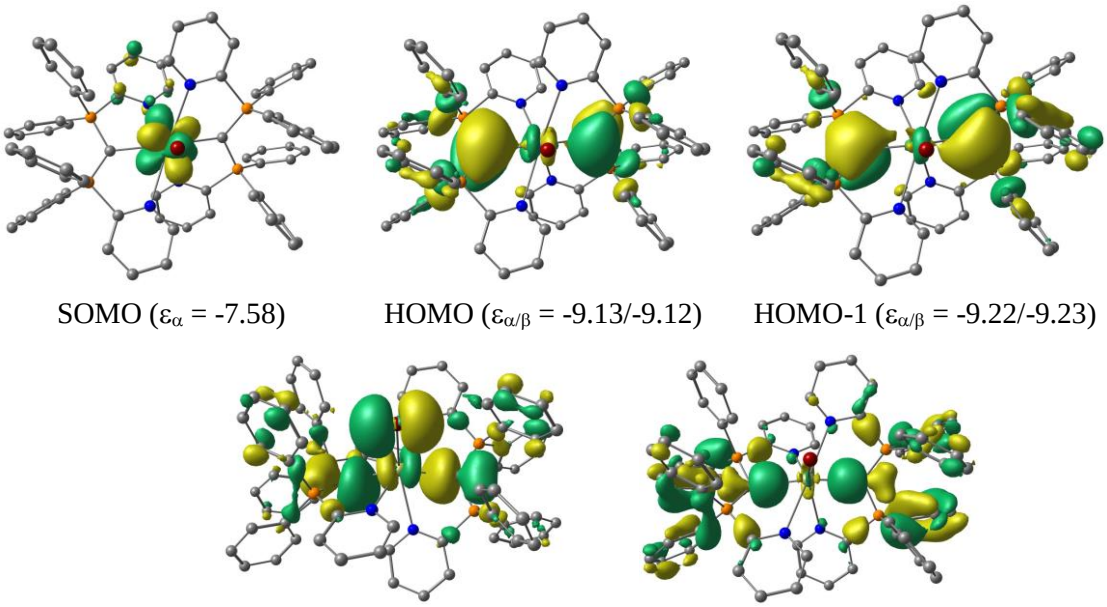

Figure S8. The shape and energy of the SOMO and relevant occupied molecular orbitals responsible for Ce-C interactions in **3**. The isosurface value is 0.025 e Å^{-3}. Energy eigenvalues are in eV.

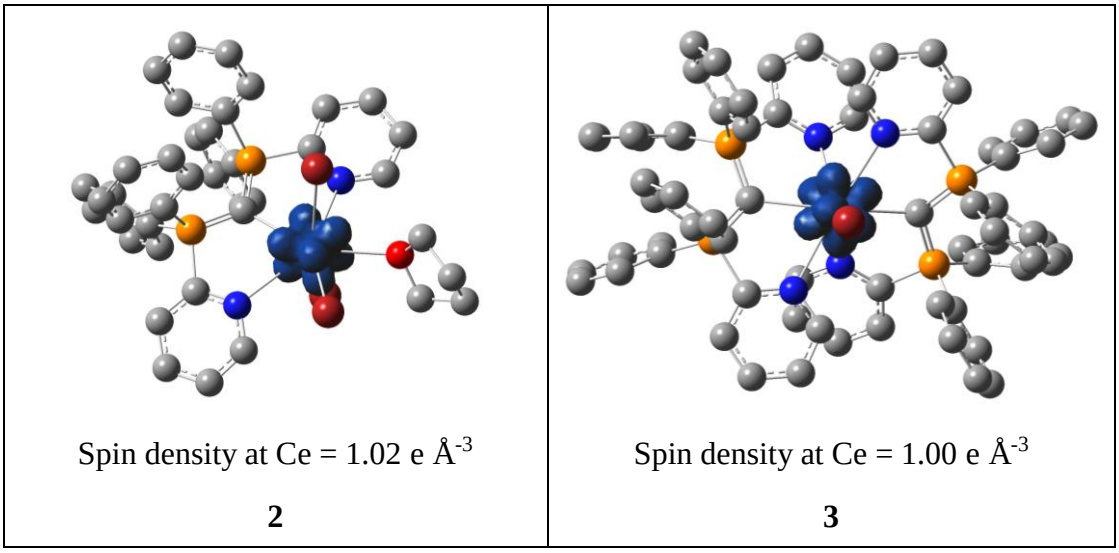

Figure S9. The shape of the spin density in **2** and **3**. The isosurface value is 0.002 e Å^{-3}.

Table S3. The ZPE uncorrected dissociation energy (D_e, kcal/mol), ZPE and BSSE corrected dissociation energy (D_0, kcal/mol), and free energy change at 298 K for the dissociation process (ΔG^{298}, kcal/mol) of **2** and **3** complexes at the BP86-D3(BJ)/def2-TZVPP/Stuttgart RSC ECP level for **2** and BP86-D3(BJ)/def2-SVP/Stuttgart RSC ECP level for **3**.

Process	D_e	D_0^{BSSE}	ΔG^{298}
2 (D) → CDP (S) + $CeBr_3$(THF) (D)	81.2	75.5	60.6
3 (D) → 2CDP (S) + $CeBr^{2+}$ (D)	420.0	401.3	384.7
3 (D) → CDP (S) + (CDP)$CeBr^{2+}$ (D)	145.1	131.6	126.0
(CDP)$CeBr^{2+}$ (D) → CDP (S) + $CeBr^{2+}$ (D)	274.9	263.8	258.7
3 (D) → 2CDP^+ (D) + CeBr (D)	260.5	243.0	225.3
3 (D) → CDP^+ (D) + (CDP)$CeBr^+$ (T)	105.7	91.3	84.4
(CDP)$CeBr^+$ (T) → CDP^+ (D) + CeBr (D)	154.7	147.4	140.9

Table S4. EDA-NOCV results for **2** at the BP86-D3(BJ)/TZ2P-ZORA level taking CDP (S) + $CeBr_3$(THF) (D) as interacting fragments. Energy values are in kcal mol^{-1}.

Energy	Interaction[c]	**2** CDP (S) + $CeBr_3$(THF) (D)
ΔE_{int}		-113.8
ΔE_{Pauli}		148.7
ΔE_{disp}[a]		-35.7 (13.6%)
ΔE_{elstat}[a]		-131.8 (50.2%)
ΔE_{orb}[a]		-95.0 (36.2%)
$\Delta E_{orb(1)}$[b]	CDP(C)→$CeBr_3$(THF) σ-donation	-29.1 (30.6%)
$\Delta E_{orb(2)}$[b]	CDP(N)→$CeBr_3$(THF) σ-donation	-9.6 (10.1%)
$\Delta E_{orb(3)}$[b]	CDP(N)→$CeBr_3$(THF) σ-donation	-9.0 (9.5%)
$\Delta E_{orb(4)}$[b]	CDP(C)→$CeBr_3$(THF) π-donation	-8.7 (9.2%)
$\Delta E_{orb(rest)}$		-38.6 (40.6%)

[a]The values in parentheses are the percentage contributions to the total attractive interactions ($\Delta E_{elstat} + \Delta E_{orb} + \Delta E_{disp}$).

[b]The values in parentheses are the percentage contributions to the total orbital interactions ΔE_{orb}.

[c]The assignment of (C) and (N) means the donation from C and N centers of CDP units, respectively.

Table S5. EDA-NOCV results for **3** at the BP86-D3(BJ)/TZ2P-ZORA level taking $(CDP)_2$ (S)+ $CeBr^{2+}$ (D) as interacting fragments. Energy values are in kcal mol^{-1}.

Energy	Interaction[c]	**3** $(CDP)_2$ (S)+ $CeBr^{2+}$ (D)
ΔE_{int}		-422.8
ΔE_{Pauli}		224.8
ΔE_{disp}[a]		-44.2 (6.8%)
ΔE_{elstat}[a]		-280.6 (43.3%)
ΔE_{orb}[a]		-322.9 (49.9%)
$\Delta E_{orb(1)}$[b]	CDP(C)→CeBr←CDP(C) σ-donation (+,+) coupled with CDP(C)→CeBr←CDP(C) π-donation	-62.6 (19.4%)
$\Delta E_{orb(2)}$[b]	CDP(C)→CeBr←CDP(C) σ-donation (+,-)	-36.8 (11.4%)
$\Delta E_{orb(3)}$[b]	CDP(C)→CeBr←CDP(C) π-donation coupled with CDP(N)→CeBr←CDP(N) σ-donation	-20.7 (6.4%)
$\Delta E_{orb(4)}$[b]	CDP(C)→CeBr←CDP(C) π-donation coupled with CDP(C)→CeBr←CDP(C) σ-donation (+,+)	-16.9 (5.2%)
$\Delta E_{orb(5)}$[b]	CDP(N)→CeBr←CDP(N) σ-donation coupled with polarization in CeBr	-18.6 (5.8%)
$\Delta E_{orb(6)}$[b]	CDP(N)→CeBr←CDP(N) σ-donation	-22.3 (6.9%)
$\Delta E_{orb(7)}$[b]	CDP(N)→CeBr←CDP(N) σ-donation coupled with CDP(C)→CeBr←CDP(C) π-donation and polarization in CeBr	-13.7 (4.2%)
$\Delta E_{orb(8)}$[b]	CDP(N)→CeBr←CDP(N) σ-donation	-12.9 (4.0%)
$\Delta E_{orb(9)}$[b]	Polarization in CeBr with slight back-donation to $(CDP)_2$	-12.6 (3.9%)
$\Delta E_{orb(rest)}$		-105.8 (32.8%)

[a]The values in parentheses are the percentage contributions to the total attractive interactions ($\Delta E_{elstat} + \Delta E_{orb} + \Delta E_{disp}$).

[b]The values in parentheses are the percentage contributions to the total orbital interactions ΔE_{orb}.

[c]The assignment of (C) and (N) means the donation from C and N centers of CDP units, respectively.

Table S6. EDA-NOCV results for **3** at the BP86-D3(BJ)/TZ2P-ZORA level taking $[(CDP)_2]^{2+}$ (S) + CeBr (D) as interacting fragments. Energy values are in kcal mol^{-1}.

Energy	**3** $[(CDP)_2]^{2+}$ (S) + CeBr (D)
ΔE_{int}	-371.6
ΔE_{Pauli}	352.2
ΔE_{disp}[a]	-44.2 (6.1%)
ΔE_{elstat}[a]	-270.1 (37.3%)
ΔE_{orb}[a]	-409.5 (56.6%)

[a]The values in parentheses are the percentage contributions to the total attractive interactions ($\Delta E_{elstat} + \Delta E_{orb} + \Delta E_{disp}$).

Table S7. The electron density ($\rho(r_c)$, au), Laplacian of electron density ($\nabla^2\rho(r_c)$, au), kinetic energy density ($G(r_c)$, au), potential energy density kinetic energy density ($V(r_c)$, au), total electronic energy density ($H(r_c)$, au) and ellipticity ($\varepsilon(r_c)$) at the bond critical points of **2**, and **3** at the BP86-D3(BJ)/def2-TZVPP/x2c-TZVPPall// BP86-D3(BJ)/def2-TZVPP/Stuttgart RSC ECP level for **2** and BP86-D3(BJ) /def2-SVP/x2c-TZVPPall//BP86-D3(BJ)/def2-SVP/Stuttgart RSC ECP level for **3**.

Complex	**BCP**	$\rho(r_c)$	$\nabla^2\rho(r_c)$	$G(r_c)$	$V(r_c)$	$H(r_c)$	$\varepsilon(r_c)$
2	Ce-C1	0.057	0.097	0.035	-0.045	-0.010	0.11
	Ce-N1	0.038	0.096	0.026	-0.029	-0.003	
	Ce-N2	0.036	0.095	0.026	-0.028	-0.002	
3	Ce-C1	0.062	0.095	0.038	-0.052	-0.014	0.19
	Ce-C2	0.062	0.097	0.038	-0.053	-0.015	0.18
	Ce-N1	0.040	0.116	0.029	-0.030	-0.001	
	Ce-N2	0.040	0.117	0.0298	-0.0303	-0.0005	
	Ce-N3	0.041	0.124	0.031	-0.032	-0.001	
	Ce-N4	0.041	0.123	0.031	-0.032	-0.001	

$\Delta\rho$	CDP	$CeBr_3(THF)$
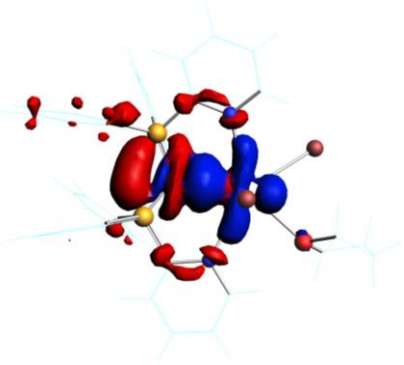 $\Delta E_{orb(1)}$ = -29.1 $\lvert\nu_{1\alpha/1\beta}\rvert$ = 0.29	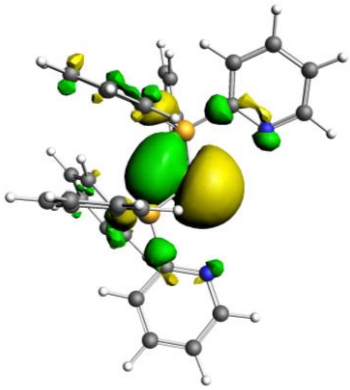 HOMO-1 (ε = -4.37) $\nu_{1\alpha/1\beta}$ = -0.10/-0.09	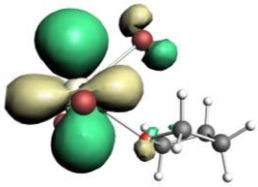 LUMO+6 (ε = -2.87) $\nu_{1\alpha/1\beta}$ = 0.07/0.07 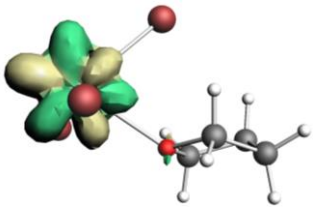 LUMO+1 (ε = -4.96) $\nu_{1\alpha/1\beta}$ = 0.02/0.02
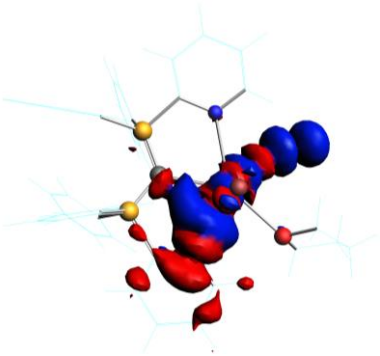 $\Delta E_{orb(2)}$ = -9.6 $\lvert\nu_{2\alpha/2\beta}\rvert$ = 0.14/0.15	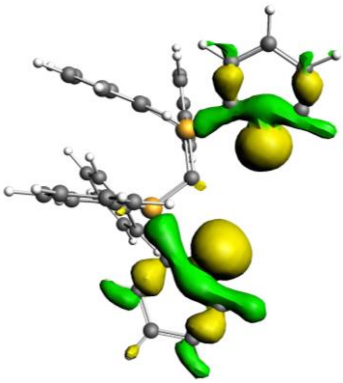 HOMO-3 (ε = -5.90) $\nu_{2\alpha/2\beta}$ = -0.01/-0.02 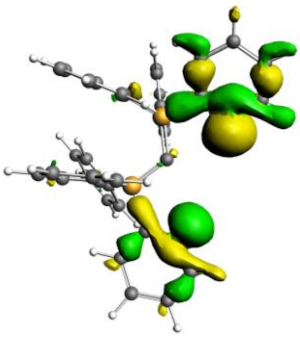 HOMO-2 (ε = -5.80) $\nu_{2\alpha/2\beta}$ = -0.01/-0.01	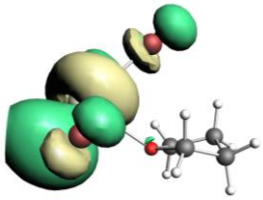 LUMO+10 (ε = -1.87) $\nu_{2\alpha/2\beta}$ = 0.02/0.01 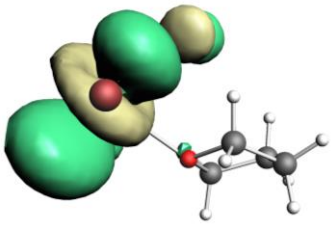 LUMO+9 (ε = -2.20) $\nu_{2\alpha/2\beta}$ = 0.01/0.01 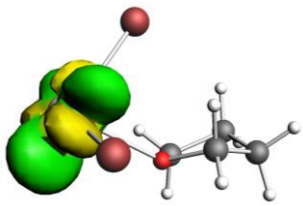 SOMO (ε = -3.84) $\nu_{2\beta}$ = 0.01

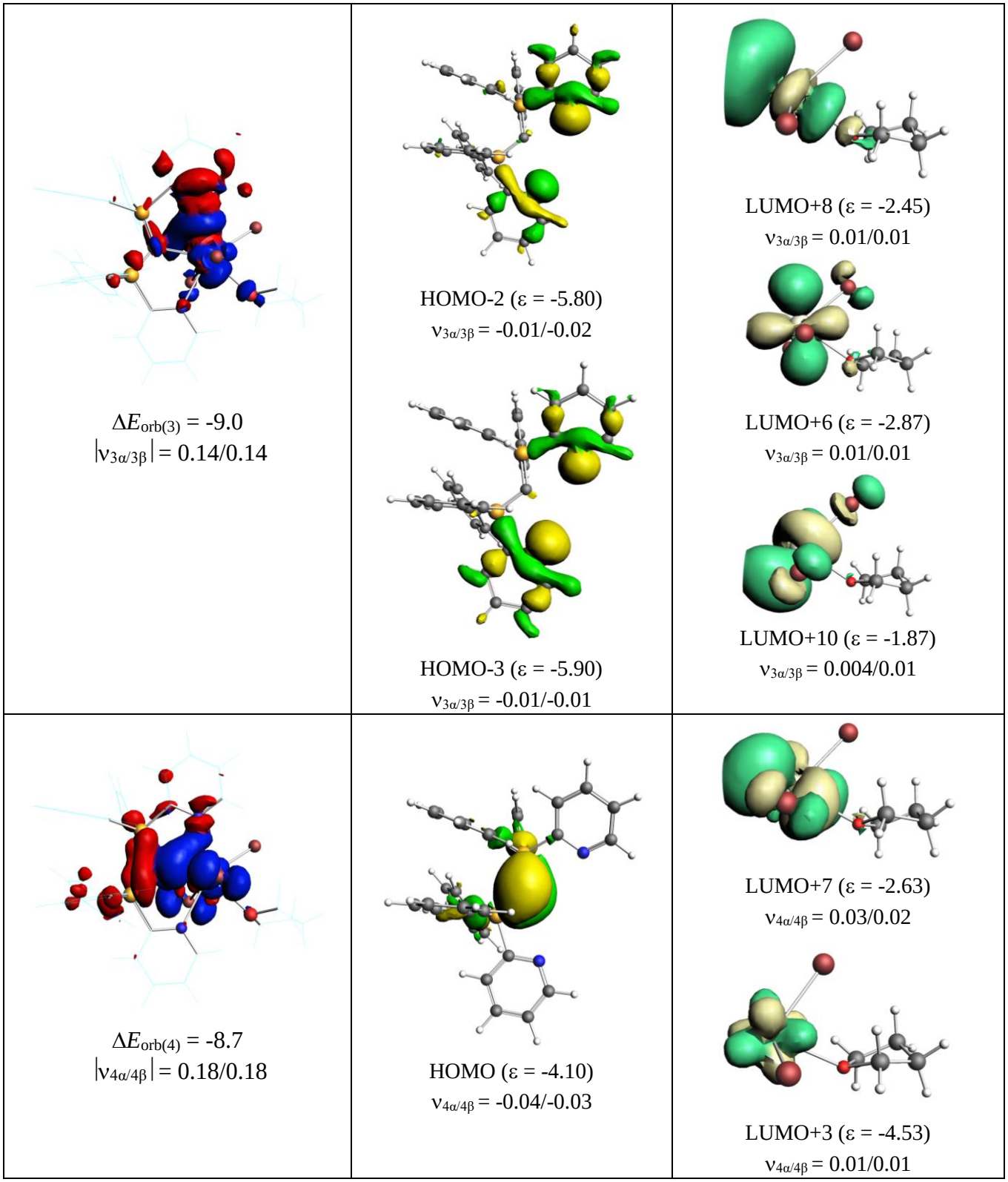

Figure S10. Shape of the deformation densities $\Delta\rho_{(1)\text{-}(4)}$ and the shape of the associated orbitals in **2** and eigenvalues $|\nu_n|$ of the charge flow. The MO energy eigen values are in eV.

$\Delta\rho$	$(CDP)_2$	$CeBr^{2+}$
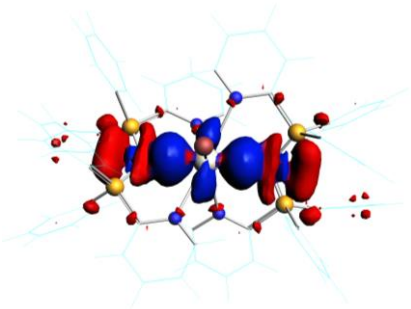 **$\Delta E_{orb(1)}$ = -62.6** **$\lvert\nu_{1\alpha/1\beta}\rvert$ = 0.34/0.35**	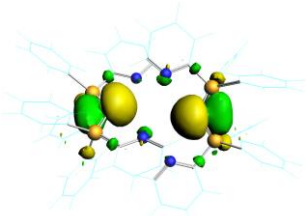 HOMO-3 (ε = -4.29) $\nu_{1\alpha/1\beta}$ = -0.08/-0.11 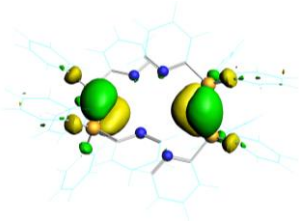 HOMO (ε = -3.99) $\nu_{1\alpha/1\beta}$ = -0.10/-0.08	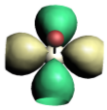 LUMO+5 (ε = -14.30) $\nu_{1\alpha/1\beta}$ = 0.15/0.14 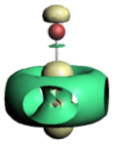 LUMO+7 (ε = -13.58) $\nu_{1\alpha/1\beta}$ = 0.01/0.01
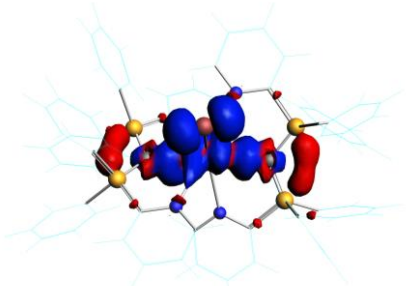 **$\Delta E_{orb(2)}$ = -36.8** **$\lvert\nu_{2\alpha/2\beta}\rvert$ = 0.32/0.31**	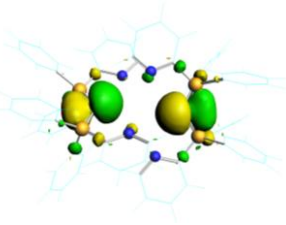 HOMO-2 (ε = -4.26) $\nu_{2\alpha/2\beta}$ = -0.08/-0.07	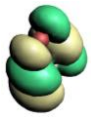 LUMO+6 (ε = -13.88) $\nu_{2\alpha/2\beta}$ = 0.05/0.05 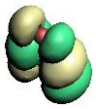 LUMO+6′ (ε = -13.88) $\nu_{2\alpha/2\beta}$ = 0.03/0.03 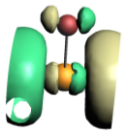 LUMO+9 (ε = -9.23) $\nu_{2\alpha/2\beta}$ = -0.03/-0.02  LUMO (ε = -16.54) $\nu_{2\alpha/2\beta}$ = 0.02/0.01

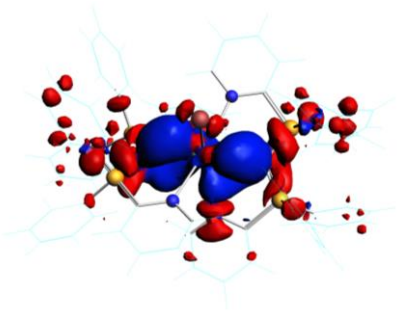 **$\Delta E_{orb(3)}$ = -20.7** **$\lvert\nu_{3\alpha/3\beta}\rvert$ = 0.23/0.21**	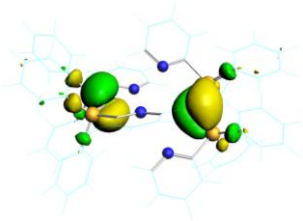 HOMO-1 (ε = -4.00) $\nu_{3\alpha/3\beta}$ = -0.06/-0.05 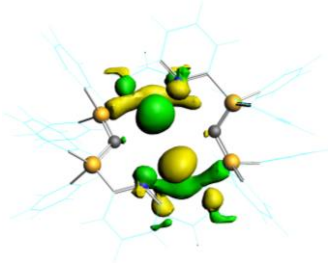 HOMO-4 (ε = -5.21) $\nu_{3\alpha/3\beta}$ = -0.02/-0.02	 LUMO+3′ (ε = -16.11) $\nu_{3\alpha/3\beta}$ = 0.03/0.03 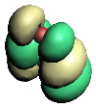 LUMO+6′ (ε = -13.88) $\nu_{3\alpha/3\beta}$ = 0.02/0.02  LUMO+3 (ε = -16.11) $\nu_{3\alpha/3\beta}$ = 0.01/0.01 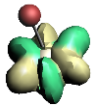 LUMO (ε = -16.54) $\nu_{3\alpha/3\beta}$ = 0.01/0.01
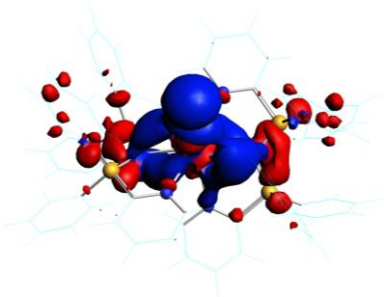 **$\Delta E_{orb(4)}$ = -16.9** **$\lvert\nu_{4\alpha/4\beta}\rvert$ = 0.19/0.21**	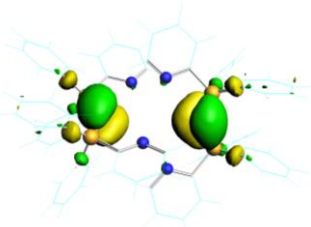 HOMO (ε = -3.99) $\nu_{4\alpha/4\beta}$ = -0.03/-0.04 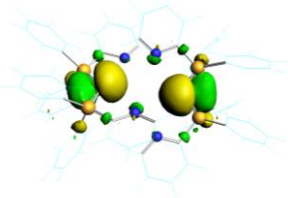 HOMO-3 (ε = -4.29) $\nu_{4\alpha/4\beta}$ = -0.01/-0.01	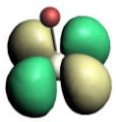 LUMO+4 (ε = -14.32) $\nu_{4\alpha/4\beta}$ = 0.03/0.02 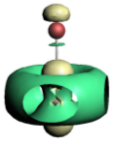 LUMO+7 (ε = -13.58) $\nu_{4\alpha/4\beta}$ = 0.004/0.02
		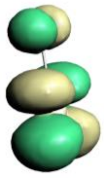

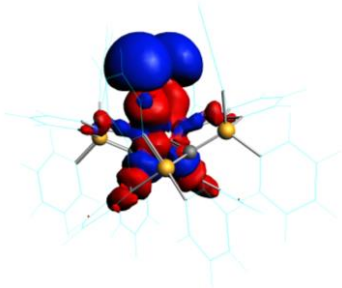 **$\Delta E_{orb(5)}$ = -18.6** **$\lvert\nu_{5\alpha/5\beta}\rvert$ = 0.24/0.25**	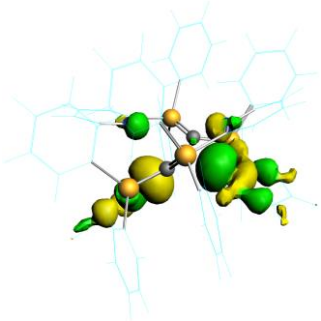 HOMO-4 (ε = -5.21) $\nu_{5\alpha/5\beta}$ = -0.04/-0.03	LUMO+6′ (ε = -13.88) $\nu_{5\alpha/5\beta}$ = 0.05/0.04  HOMO (ε = -17.03) $\nu_{5\alpha/5\beta}$ = -0.04/-0.04 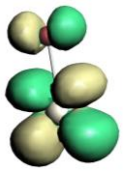 LUMO+6 (ε = -13.88) $\nu_{5\alpha/5\beta}$ = 0.03/0.03
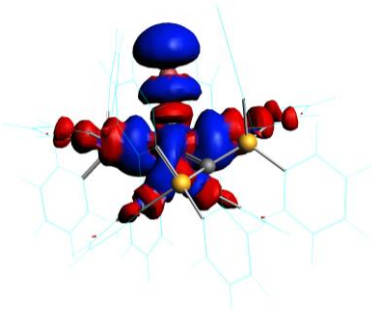 **$\Delta E_{orb(6)}$ = -22.3** **$\lvert\nu_{6\alpha/6\beta}\rvert$ = 0.21/0.21**	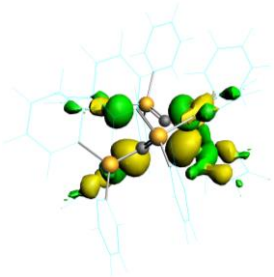 HOMO-5 (ε = -5.29) $\nu_{6\alpha/6\beta}$ = -0.04/-0.05 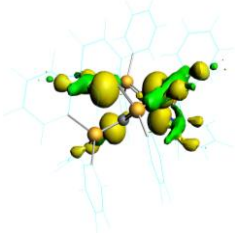 HOMO-7 (ε = -5.74) $\nu_{6\alpha/6\beta}$ = -0.01/-0.01	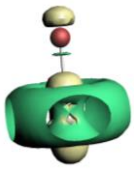 LUMO+7 (ε = -13.58) $\nu_{6\alpha/6\beta}$ = 0.03/0.02 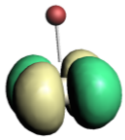 LUMO+4 (ε = -13.32) $\nu_{6\alpha/6\beta}$ = 0.03/0.04  LUMO+8 (ε = -12.21) $\nu_{6\alpha/6\beta}$ = 0.01/0.01
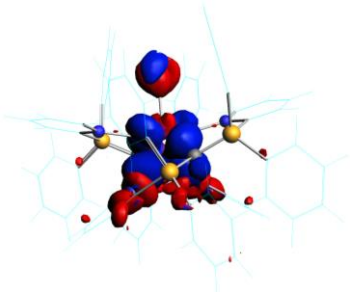 **$\Delta E_{orb(7)}$ = -13.7**	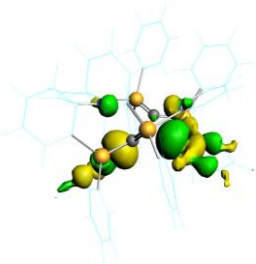 HOMO-4 (ε = -5.21) $\nu_{7\alpha/7\beta}$ = -0.03/-0.02	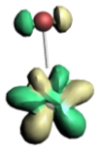 LUMO+3 (ε = -16.11) $\nu_{7\alpha/7\beta}$ = 0.02/0.02

$\lvert\nu_{7\alpha/7\beta}\rvert$ = 0.18/0.17	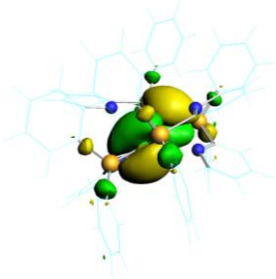 HOMO-1 (ε = -4.00) $\nu_{7\alpha/7\beta}$ = -0.01/-0.02	 HOMO (ε = -17.03) $\nu_{7\alpha/7\beta}$ = -0.01/-0.01 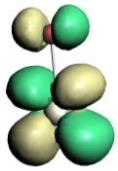 LUMO+6 (ε = -13.88) $\nu_{7\alpha/7\beta}$ = 0.01/0.01 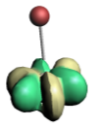 LUMO (ε = -16.54) $\nu_{7\alpha/7\beta}$ = 0.01/0.01
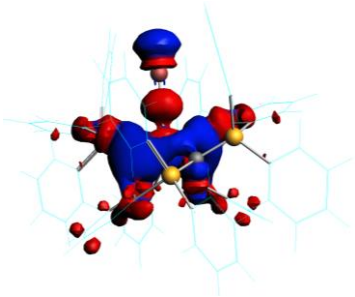 **$\Delta E_{orb(8)}$ = -12.9** **$\lvert\nu_{8\alpha/8\beta}\rvert$ = 0.13/0.13**	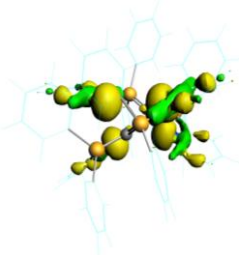 HOMO-7 (ε = -5.74) $\nu_{8\alpha/8\beta}$ = -0.02/-0.02	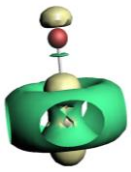 LUMO+7 (ε = -13.58) $\nu_{8\alpha/8\beta}$ = 0.02/0.02  LUMO+8 (ε = -12.21) $\nu_{8\alpha/8\beta}$ = 0.01/0.01
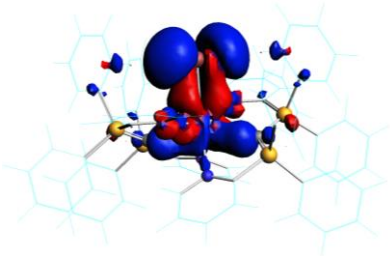 **$\Delta E_{orb(9)}$ = -12.6** **$\lvert\nu_{9\alpha/9\beta}\rvert$ = 0.22/0.22**	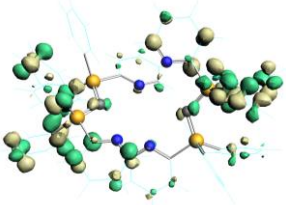 LUMO+8 (ε = -1.83) $\nu_{8\alpha/8\beta}$ = 0.004/0.005	 HOMO′ (ε = -17.03) $\nu_{7\alpha/7\beta}$ = -0.04/-0.03 

		LUMO+3 (ε = -16.11) $\nu_{9\alpha/9\beta}$ = 0.01/0.01 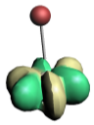 LUMO (ε = -16.54) $\nu_{9\alpha/9\beta}$ = 0.01/0.01  LUMO+3′ (ε = -16.11) $\nu_{9\alpha/9\beta}$ = 0.01/0.01 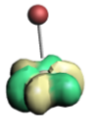 LUMO′ (ε = -16.54) $\nu_{9\alpha/9\beta}$ = 0.01/0.01

Figure S11. Shape of the deformation densities $\Delta\rho_{(1)\text{-}(9)}$ and the shape of the associated orbitals in **3** and eigenvalues $|\nu_n|$ of the charge flow. The MO energy eigen values are in eV.

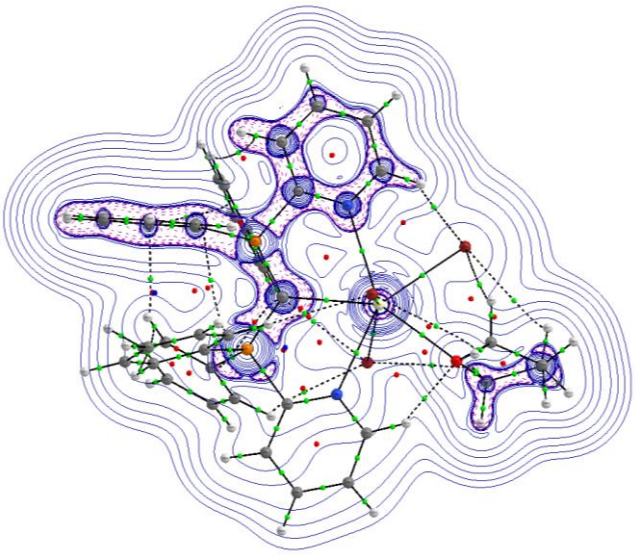

2 (at C1-Ce1-N1 plane)

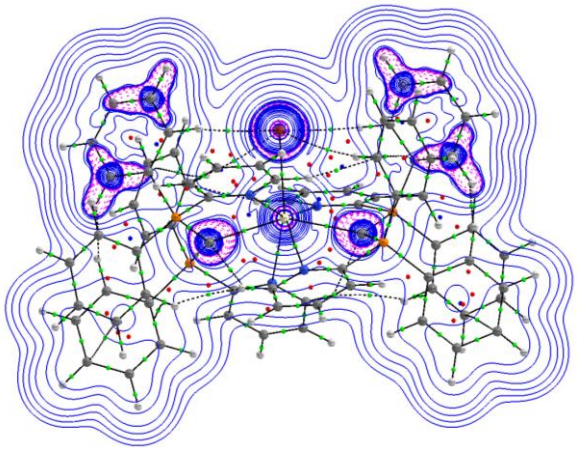

3 (at C1-Ce1-C2 plane)

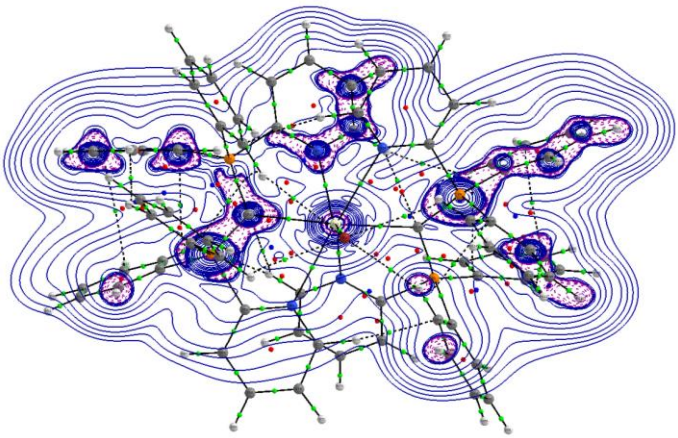

3 (at C1-Ce-N1 plane)

Figure S12. The contour plots of Laplacian of electron density at the mentioned plane of **2** and **3** complexes.

Table S8. The Cartesian coordinates of **2** and **3**.

2

E = -10575.0032 au

Ce	-1.763986795	0.194171604	-0.082960901
Br	-1.546161765	-0.439433018	2.749857054
Br	-3.742297467	2.277757170	0.355662326
Br	-1.702130425	-0.562148601	-2.863546087
P	1.697228519	1.405803352	-0.228994812
P	1.500402745	-1.449882124	0.253096778
O	-4.016964351	-1.088731765	-0.113945419
N	-0.599208201	2.403873629	-1.195377162
N	-1.035048579	-2.407627914	0.077322195
C	-1.375928270	3.227328611	-1.923086020
H	-2.449109314	3.042311607	-1.856522560
C	-0.854398865	4.266153256	-2.695605993
H	-1.528736630	4.896228345	-3.274650361
C	0.523937126	4.475118245	-2.708106223
H	0.962893880	5.278793275	-3.300704164
C	1.336282363	3.627675325	-1.952660853
H	2.420143231	3.739465665	-1.947551784
C	0.734240662	2.602095372	-1.220656039
C	2.067479599	2.253017938	1.340157412
C	2.841669497	3.423353586	1.410883115
H	3.257041421	3.866719992	0.504347270
C	3.083185586	4.021211639	2.647757045
H	3.685179138	4.929291922	2.704055414
C	2.548400429	3.458801011	3.814006133
H	2.738386211	3.930665607	4.779241940
C	1.761750915	2.306985593	3.740466445
H	1.323757484	1.874773936	4.640452305
C	1.516231712	1.703743368	2.505478751
H	0.875707425	0.821948160	2.438514466
C	3.278231816	1.248567096	-1.121657983
C	4.526383699	1.357350068	-0.492338408
H	4.582825924	1.679806770	0.547291156
C	5.693729760	1.041139044	-1.193306825
H	6.661851388	1.122706844	-0.697097737
C	5.619931389	0.617712884	-2.522597720
H	6.530775930	0.361808629	-3.065275371
C	4.377001724	0.518318574	-3.157614663
H	4.315008128	0.179387361	-4.191730975
C	3.210684986	0.829649367	-2.462064224
H	2.237363991	0.724333950	-2.943937165
C	0.776047336	0.017456297	-0.091746564

C	2.439495804	-1.528838248	1.807176109
C	1.767223359	-1.861566709	2.995172006
H	0.738243025	-2.220167577	2.960435298
C	2.390262693	-1.660406275	4.228055151
H	1.852720564	-1.904377519	5.144991210
C	3.681041014	-1.127765223	4.288598230
H	4.159642344	-0.962583084	5.254702359
C	4.353107641	-0.793604014	3.108530769
H	5.356792710	-0.368308725	3.150314091
C	3.735038578	-0.987503856	1.873686879
H	4.249699532	-0.690121212	0.960573105
C	2.521927559	-2.115536091	-1.106373804
C	3.809023792	-2.649904097	-0.973002780
H	4.282824414	-2.707300408	0.006406233
C	4.489320738	-3.113759596	-2.103727643
H	5.500301400	-3.510501030	-2.000659827
C	3.874650206	-3.076702567	-3.357399585
H	4.406376205	-3.446527221	-4.235430024
C	2.575707515	-2.570207538	-3.486017428
H	2.086576559	-2.547771385	-4.460772107
C	1.902080287	-2.078251479	-2.370016175
H	0.897846651	-1.652648833	-2.471524400
C	0.228256573	-2.758825714	0.374614318
C	0.599703648	-4.073369831	0.670508189
H	1.640075698	-4.306471440	0.898002938
C	-0.379935200	-5.064668432	0.660183528
H	-0.124761155	-6.098547287	0.895272743
C	-1.688272792	-4.707004562	0.330607284
H	-2.485257423	-5.449347452	0.295490365
C	-1.971458202	-3.372355716	0.044241157
H	-2.976800284	-3.035336866	-0.210621483
C	-4.811930023	-1.095200263	1.122050330
H	-4.303270029	-0.455040957	1.853008506
H	-4.825028674	-2.131395088	1.497269137
C	-6.193548573	-0.598573829	0.717699972
H	-6.210671955	0.499434554	0.755663963
H	-6.982588523	-0.992736937	1.371147392
C	-6.309125065	-1.081332591	-0.736629669
H	-6.568682431	-2.150541240	-0.775753807
H	-7.056233010	-0.524035217	-1.316164230
C	-4.898569896	-0.847044328	-1.262039668
H	-4.575582461	-1.519704368	-2.065035817
H	-4.755562264	0.195467583	-1.584009818

3

E = -7332.739012 au

Ce	-0.000043980	0.000166026	-0.212452018
Br	0.000364020	0.000252026	-3.046446223
P	-3.158414191	-1.344793105	0.896223061
P	-3.422292242	1.314292080	-0.328250027
P	3.158343234	1.344714157	0.896292060
P	3.422221279	-1.314344029	-0.328311026
N	-0.586031005	-1.792233107	1.659269116
N	-0.976771077	2.425675192	-0.786230061
N	0.585840041	1.792717161	1.659003114
N	0.976610118	-2.425709139	-0.785794062
C	0.437978078	-2.436866142	2.260041157
H	1.427856142	-1.966542098	2.133771152
C	0.258898079	-3.631834235	2.970591209
H	1.120158146	-4.123199256	3.446329245
C	-1.031192010	-4.184322287	3.047078214
H	-1.206979008	-5.127315356	3.587358258
C	-2.097403091	-3.511805251	2.428855171
H	-3.122890163	-3.906793289	2.477259173
C	-1.831667089	-2.307083163	1.754910125
C	-3.695888220	-2.431188192	-0.481604038
C	-3.143579183	-2.180421164	-1.756216129
H	-2.457306143	-1.331593096	-1.910350142
C	-3.490893198	-2.994383230	-2.844513206
H	-3.061155170	-2.782104211	-3.834897278
C	-4.391822254	-4.059014315	-2.665761195
H	-4.673797267	-4.692454363	-3.520950254
C	-4.940291289	-4.314235338	-1.395075104
H	-5.647022354	-5.146858406	-1.256623095
C	-4.593000272	-3.505874275	-0.300138024
H	-5.035087302	-3.704975294	0.688560044
C	-4.535267294	-1.267476118	2.094354147
C	-5.866129411	-1.151860123	1.638898115
H	-6.096896412	-1.292291134	0.572573038
C	-6.896828471	-0.863529115	2.546540180
H	-7.932348547	-0.770395120	2.185964153
C	-6.607168434	-0.699387095	3.911996276
H	-7.417759498	-0.478353091	4.623022329
C	-5.283498354	-0.823118092	4.371676312
H	-5.057921338	-0.703206083	5.442495400
C	-4.246927273	-1.095699103	3.466309248
H	-3.208561197	-1.166582094	3.827658271

C	-2.443621159	0.126678008	0.419777027
C	-4.717895342	2.040355122	0.739963052
C	-4.518884326	1.987795121	2.135656150
H	-3.618015258	1.494207095	2.530732180
C	-5.482944386	2.521020147	3.002525215
H	-5.331744370	2.465106147	4.091066290
C	-6.646571501	3.114052178	2.480372175
H	-7.406452568	3.527883196	3.160971223
C	-6.842997492	3.178001179	1.089601076
H	-7.753469597	3.642980200	0.681465047
C	-5.882003458	2.643229151	0.215537012
H	-6.047887455	2.682660153	-0.872094065
C	-4.233986297	0.852456038	-1.898870139
C	-5.477702356	0.182479978	-1.882894140
H	-6.045855415	0.097143966	-0.945002070
C	-5.992043433	-0.370000067	-3.064551223
H	-6.961827471	-0.890045118	-3.048466225
C	-5.268278359	-0.259927051	-4.265651311
H	-5.672919389	-0.695434088	-5.192125377
C	-4.032317276	0.409591010	-4.284885311
H	-3.462429236	0.497364024	-5.222254380
C	-3.511126243	0.965498057	-3.105916226
H	-2.524910177	1.453263101	-3.126358226
C	-2.298995175	2.707709197	-0.778171057
C	-2.802651227	3.976436280	-1.109956085
H	-3.885750307	4.165965282	-1.082879080
C	-1.897535173	4.989270364	-1.464479108
H	-2.260584209	5.994402452	-1.728131126
C	-0.524156070	4.695045358	-1.476761111
H	0.223045975	5.453338401	-1.752275129
C	-0.110455026	3.401583271	-1.130753084
H	0.959511057	3.134890262	-1.139029083
C	-0.438006039	2.437496197	2.259890162
H	-1.428030104	1.967547154	2.133383149
C	-0.258591039	3.632131283	2.970910208
H	-1.119724104	4.123598308	3.446772246
C	1.031680049	4.184154337	3.047719217
H	1.207737050	5.126880409	3.588378257
C	2.097715131	3.511508303	2.429344174
H	3.123322199	3.906149344	2.477981177
C	1.831653124	2.307099212	1.754949125
C	3.696014259	2.431252244	-0.481356038
C	3.143779223	2.180611218	-1.756035129
H	2.457520184	1.331791151	-1.910280142

C	3.491164237	2.994681279	-2.844223206
H	3.061498209	2.782507259	-3.834661281
C	4.392082291	4.059300368	-2.665306193
H	4.674099305	4.692830418	-3.520414256
C	4.940481327	4.314380391	-1.394566104
H	5.647212381	5.146979461	-1.255974096
C	4.593121311	3.505903327	-0.299730025
H	5.035181342	3.704895346	0.689003045
C	4.535059332	1.267209169	2.094581148
C	5.865963408	1.151694173	1.639213113
H	6.096823439	1.292345189	0.572937038
C	6.896587483	0.863186166	2.546884183
H	7.932138570	0.770123171	2.186380155
C	6.606817483	0.698778150	3.912286281
H	7.417356529	0.477608142	4.623329331
C	5.283112393	0.822433146	4.371881310
H	5.057436378	0.702324135	5.442657381
C	4.246616313	1.095184150	3.466478246
H	3.208222238	1.166002147	3.827764270
C	2.443582195	-0.126698956	0.419671027
C	4.234058334	-0.852450990	-1.898832138
C	5.477792422	-0.182507927	-1.882641140
H	6.045816467	-0.097261914	-0.944663073
C	5.992300454	0.370047119	-3.064189224
H	6.962094494	0.890067169	-3.047946223
C	5.268685397	0.260077103	-4.265389310
H	5.673453434	0.695644140	-5.191780374
C	4.032720313	-0.409424959	-4.284841310
H	3.462959275	-0.497119972	-5.222294380
C	3.511364282	-0.965413002	-3.105981225
H	2.525157218	-1.453187053	-3.126569231
C	4.717728382	-2.040589071	0.739894053
C	5.881784485	-2.643532099	0.215454013
H	6.047755478	-2.682801100	-0.872169066
C	6.842660565	-3.178555127	1.089505078
H	7.753087637	-3.643600152	0.681345046
C	6.646166521	-3.114757126	2.480266175
H	7.405941594	-3.528777146	3.160870225
C	5.482590419	-2.521623097	3.002437213
H	5.331374422	-2.465811090	4.090981294
C	4.518644365	-1.988179065	2.135588151
H	3.617804296	-1.494538043	2.530660180
C	2.298841216	-2.707674145	-0.778345061
C	2.802448266	-3.976259228	-1.110751084

H	3.885569344	-4.165729231	-1.084152079
C	1.897255211	-4.989020311	-1.465273107
H	2.260257247	-5.994035362	-1.729440125
C	0.523849109	-4.694885308	-1.476871111
H	-0.223413936	-5.453140382	-1.752328131
C	0.110210066	-3.401570216	-1.130245085
H	-0.959780016	-3.134968210	-1.137944084

5. References

1. W. Su, S. Pan, X. Sun, S. Wang, L. Zhao, G. Frenking, C. Zhu, *Nat. Comm.* 2018, **9**, 4997.

2. (a) G. Sheldrick, *Acta Crystallogr. Section C* 2015, **71**, 3-8； (b) G. Sheldrick, *Acta Crystallogr. Section A* 2008, **64**, 112-122; (c) O. V. Dolomanov, L. J. Bourhis, J. A. K. Howard, H. Puschmann, *J. Applied Crystallogr.* 2009, **42**, 339-341.

3. (a) A. D. Becke, *Phys. Rev. A*, 1988, **38**, 3098-3100; (b) J. P. Perdew, *Phys. Rev. B*, 1986, **33**, 8822-8824; (c) S. Grimme, S. Ehrlich, L. Goerigk, *J. Comput. Chem*. 2011, **32**, 1456-1465; (d) S. Grimme, J. Antony, S. Ehrlich, H. Krieg, *J. Chem. Phys*. 2010, **132**, 154104-154119.

4. (a) F. Weigend, R. Ahlrichs, *Phys. Chem. Chem. Phys*. 2005, **7**, 3297-3305; (b) F. Weigend, *Phys. Chem. Chem. Phys*. 2006, **8**, 1057-1065; (c) M. Dolg, H. Stoll, H. Preuss, R.M. Pitzer, *J. Phys. Chem*. 1993, **97**, 5852-5859.

5. S. F. Boys, F. Bernardi, *Mol. Phys.*, 1970, **19**, 553-566.

6. Gaussian 16, Revision A.03, M. J. Frisch, G. W. Trucks, H. B. Schlegel, G. E. Scuseria, M. A. Robb, J. R. Cheeseman, G. Scalmani, V. Barone, G. A. Petersson, H. Nakatsuji, X. Li, M. Caricato, A. V. Marenich, J. Bloino, B. G. Janesko, R. Gomperts, B. Mennucci, H. P. Hratchian, J. V. Ortiz, A. F. Izmaylov, J. L. Sonnenberg, D. Williams-Young, F. Ding, F. Lipparini, F. Egidi, J. Goings, B. Peng, A. Petrone, T. Henderson, D. Ranasinghe, V. G. Zakrzewski, J. Gao, N. Rega, G. Zheng, W. Liang, M. Hada, M. Ehara, K. Toyota, R. Fukuda, J. Hasegawa, M. Ishida, T. Nakajima, Y. Honda, O. Kitao, H. Nakai, T. Vreven, K. Throssell, J. A. Montgomery, Jr., J. E. Peralta, F. Ogliaro, M. J. Bearpark, J. J. Heyd, E. N. Brothers, K. N. Kudin, V. N. Staroverov, T. A. Keith, R. Kobayashi, J. Normand, K. Raghavachari, A. P. Rendell, J. C. Burant, S. S. Iyengar, J. Tomasi, M. Cossi, J. M. Millam, M. Klene, C. Adamo, R. Cammi, J. W. Ochterski, R. L. Martin, K. Morokuma, O. Farkas, J. B. Foresman, and D. J. Fox, Gaussian, Inc., Wallingford CT, 2016.

7. NBO 7.0. E. D. Glendening, J. K. Badenhoop, A. E. Reed, J. E. Carpenter, J. A. Bohmann, C. M. Morales, P. Karafiloglou, C. R. Landis, F. Weinhold, Theoretical Chemistry Institute, University of Wisconsin, Madison, WI, **2018**.

8. P. Pollak, F. Weigend, *J. Chem. Theory Comput*. 2017, **13,** 3696-3705.

9. AIMAll (Version 17.11.14), T. A. Keith, TK Gristmill Software, Overland Park KS, USA, **2017** (aim.tkgristmill.com).

10. (a) A. Michalak, M. Mitoraj, T. Ziegler, *J. Phys. Chem. A* 2008, **112**, 1933-1939; (b) M. P.

Mitoraj, A. Michalak, T. Ziegler, *J. Chem. Theory Comput.* 2009, **5**, 962-975.

11. (a) ADF2017, SCM, Theoretical Chemistry, Vrije Universiteit, Amsterdam, The Netherlands, http://www.scm.com; (b) G. T. Velde, F. M. Bickelhaupt, E. J. Baerends, C. F. Guerra, S. J. A. Van Gisbergen, J. G. Snijders, T. Ziegler, *J. Comput. Chem*. 2001, **22**, 931-967.

12. E. Van Lenthe, E. J. Baerends, *J. Comput. Chem*. 2003, **24**, 1142-1156.

13. E. Van Lenthe, A. Ehlers, E. J. Baerends, *J. Chem. Phys*. **1999**, 110, 8943-8953.

14. (a) L. Zhao, M. Von Hopffgarten, D. M. Andrada, G. Frenking, *WIREs Comput. Mol. Sci.*, 2018, **8**, e1345; (b) G. Frenking, F. M. Bickelhaupt, *The EDA Perspective of Chemical Bonding* in *The Chemical Bond. Fundamental Aspects of Chemical Bonding*, G. Frenking and S. Shaik (Eds), Wiley-VCH, Weinheim, 2014, **121**; (c) G. Frenking, R. Tonner, S. Klein, N. Takagi, T. Shimizu, A. Krapp, K. K. Pandey, P. Parameswaran, *Chem. Soc. Rev*. 2014, **43**, 5106-5139; (d) L. Zhao, M. Hermann, N. Holzmann, G. Frenking, *Coord. Chem. Rev*. 2017, **344**, 163-204; (e) G. Frenking, M. Hermann, D. M. Andrada, N. Holzmann, *Chem. Soc. Rev*. 2016, **45**, 1129-1144.